

Stepwise Sarcomere Shortening: Analysis by High-Speed Cinemicrography

Abstract. Sarcomere shortening in striated muscle appears to follow a regionally synchronized staircase-like time course not anticipated in some cross-bridge models. The visualization method used has been criticized as subject to Bragg diffraction effects. Two independent optical methods were used to visualize a muscle during contraction; agreement between the stepwise behavior observed with the two methods suggests that the phenomenon is genuine.

We recently reported that records of sarcomere shortening in striated muscle fibers show periods of shortening, or "bursts," alternating with periods of virtually no motion, or "pauses" (Fig. 1A) (1). The presence of this staircase-like behavior implies a possible synchronization of activity over relatively large regions of a muscle fiber. Since cross-bridge models of muscle contraction usually assume that the cross bridges function independently, this synchronous behavior is not necessarily anticipated in these models.

Although a number of potential artifacts have been ruled out, it has re-

mained possible that this discontinuous shortening pattern, obtained by laser diffraction, does not reflect the actual shortening behavior. In particular, it has been suggested that stepwise shortening may be accounted for by Bragg scattering of the incident light by skewed myofibrillar planes (2).

To summarize this argument, assume the presence of two regions in a muscle fiber, both illuminated by plane-coherent monochromatic light, and with region 1 having a longer sarcomere length (SL) than region 2. At some initial stage during contraction, suppose that a large part of region 2 satisfies the criterion for Bragg scattering but that only a small part of 1 does. The resultant first-order diffraction peak may be idealized as in Fig. 1B. Suppose further that both regions 1 and 2 subsequently undergo smooth shortening at the same rate and that, as this occurs, progressively less of region 2 satisfies the Bragg criterion, whereas the contribution from region 1 gradually increases. The sequence is shown in Fig. 1, C to E. It can be seen that, if the changes in the relative intensities are complementary to each other, the median of the first order—and hence the observed average SL—can remain constant despite the smooth shortening of the two contributing regions. A pause in the average SL is therefore seen.

Although this mechanism may describe the behavior of any diffraction order, it is to be expected that individual orders will behave independently, since each order results from a different and independent set of skewed planes. Given the fortuity required to obtain a pause in one first order, for example, it is highly unlikely that the other diffraction orders would show the same behavior. Thus an image obtained from the collection of all orders should not show the pause in question if it is only due to Bragg diffraction. This report describes the results of experiments in which the behavior of such an image was compared with that of a single diffraction order during pauses.

The specimen was illuminated with coherent light (Spectra-Physics 5-mW He-Ne laser) and the diffraction orders were collected by a microscope (Fig. 2).

The image thus formed was not, however, a conventional striation image. The depth of field for the microscope was essentially infinite since coherent light was used, and the Fourier plane of the objective contained all diffraction peaks up to the third order inclusive, derived from the entire illuminated volume of the fiber. The image just beyond the ocular, theoretically the Fourier transform of the entire diffraction pattern at the previous Fourier plane, consisted of a banded pattern whose characteristic spacing was therefore derived from all diffraction order positions and constituted a "composite" SL. On-line monitoring of the diffraction pattern by a video system showed that, although the intensities of the various orders varied with time, the two first-order peaks never disappeared during the early stages of contraction, when all records were taken.

A high-speed rotating prism camera (Hycam) was used to record the banding pattern at one ocular at a rate of 4000 frames per second. The position of a single first-order diffraction peak could be monitored simultaneously with the filming, allowing on-line computation of SL (3).

Films were taken of contractions of single fibers of frog semitendinosus and toe muscles. The toe fibers proved most satisfactory, since their short lengths (about 1 mm) obviated the serious axial translation suffered during contraction by most regions of the longer semitendinosus fibers. Four films were chosen for analysis on the basis of good contrast, clear and uniform band patterns,

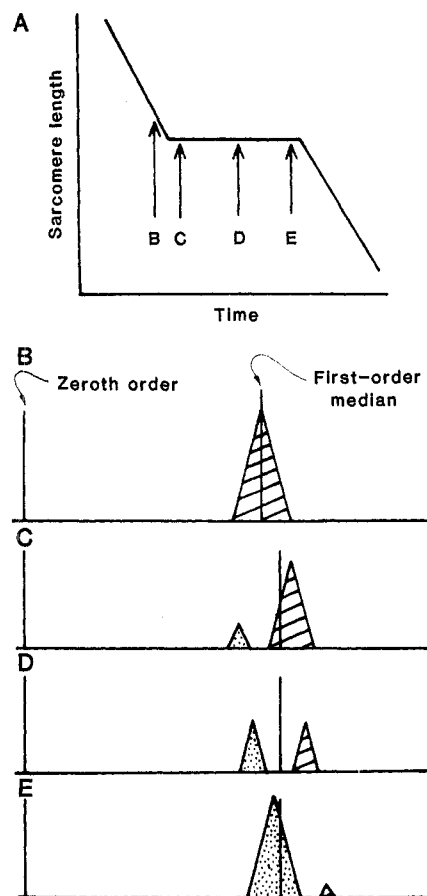


Fig. 1. (A) Behavior of sarcomere length with time during a contraction, and a pause. The first-order diffraction intensities, at the times shown by B through E, are idealized in the corresponding panels (B) through (E). The stippled subpeak is contributed by region 1 (see text); the hatched peak, by region 2.

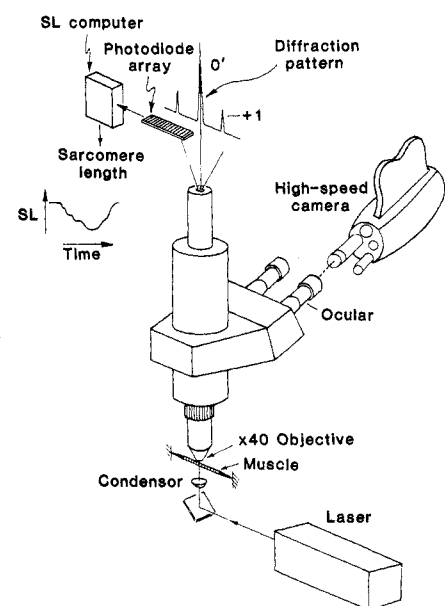


Fig. 2. Schematic of the apparatus used. The laser beam was focused to a diameter of about 50 μm at the specimen.

and absence of significant lateral translation.

A scanning microdensitometer was constructed to provide measurements of striation spacing with a resolution of 0.2 percent. The output of an intensity scan across about 35 bands was recorded on an X-Y recorder and the average band spacing was calculated by dividing the distance between the first and last bands

by the number of bands less one. Visual inspection of the image during each scan ensured that spurious bands due to optical noise and nonsarcomeric scatterers were not counted. About ten scan lines per film frame were so analyzed; the individual scan lines were distributed uniformly across the fiber width or, when striations were obscured or noisy in some regions, were distributed uni-

formly over the remaining regions of the frame. The resulting ten values of band spacing were averaged to give a grand mean SL for each frame; typically, the standard error was between 0.1 and 0.4 percent. There was significant variation (1 to 4 percent) in SL across the width of the muscle; thus if the positions of the individual scan lines across the muscle width had varied from frame to frame,

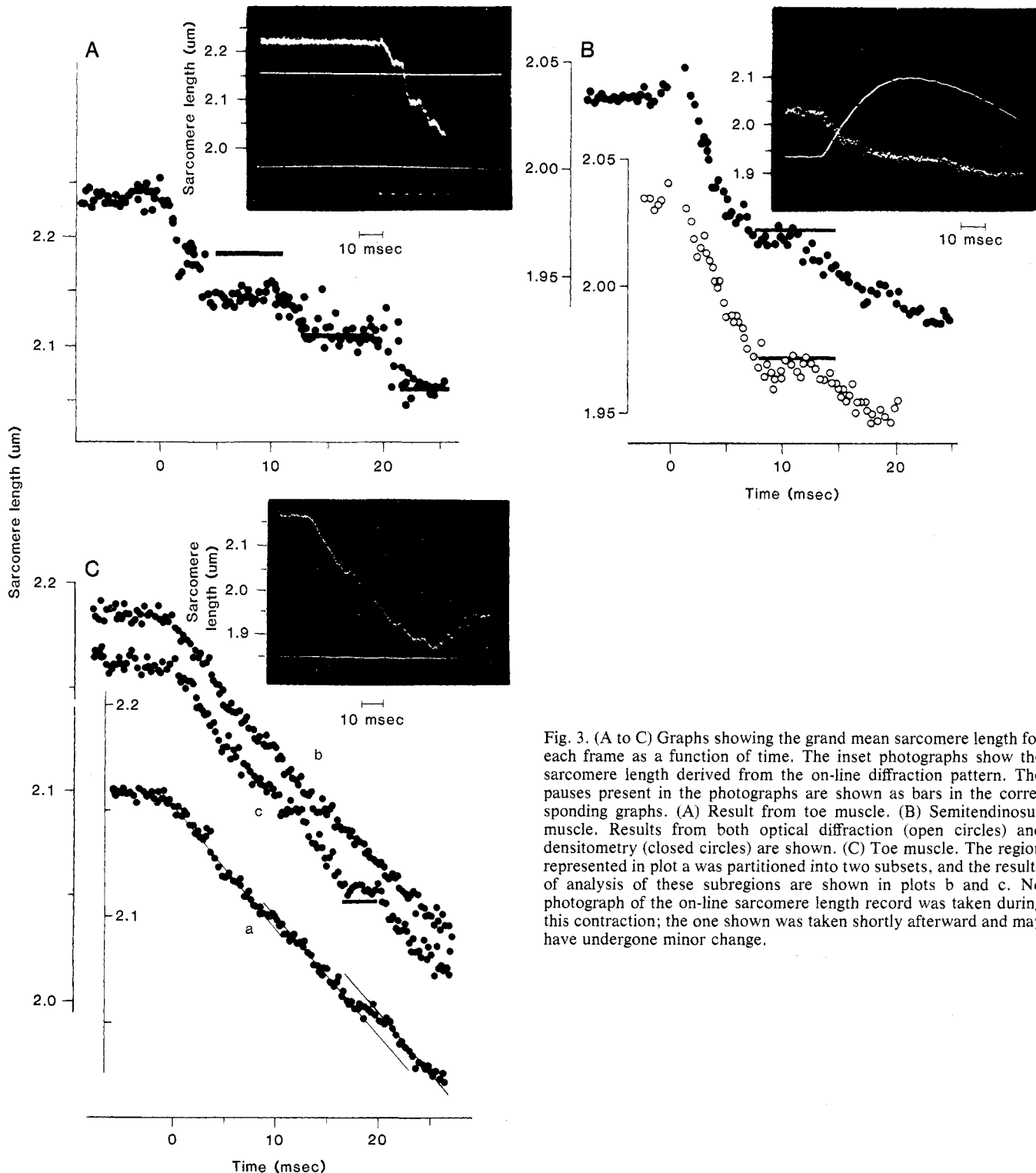


Fig. 3. (A to C) Graphs showing the grand mean sarcomere length for each frame as a function of time. The inset photographs show the sarcomere length derived from the on-line diffraction pattern. The pauses present in the photographs are shown as bars in the corresponding graphs. (A) Result from toe muscle. (B) Semitendinosus muscle. Results from both optical diffraction (open circles) and densitometry (closed circles) are shown. (C) Toe muscle. The region represented in plot a was partitioned into two subsets, and the results of analysis of these subregions are shown in plots b and c. No photograph of the on-line sarcomere length record was taken during this contraction; the one shown was taken shortly afterward and may have undergone minor change.

large fluctuations would have arisen in the grand mean SL. Hence a consistent set of scan lines was used throughout the analysis of each film. The resulting grand mean SL was plotted as a function of time from the onset of the contraction.

Two precautions were taken to ensure objectivity of the analysis: each film was processed by a different analyst, and the densitometer tracings were processed in random order so that the analyst had no knowledge of the frame number until the results were plotted. The results for three of the four films are shown in Fig. 3; the fourth result is omitted due to space limitations. Each graph shows SL (mean band spacing) as computed from the film and a photographic record of SL as computed from a single first order. The pauses in the on-line diffraction records are shown as bars in the graph. For all four films, these pauses corresponded to those present in the microdensitometry results, with matching onset times and durations and at similar SL's. This supports the hypothesis that stepwise shortening is a real phenomenon and not an artifact arising from the analysis of a single diffraction order.

One film was also analyzed by optical diffraction; each frame was completely illuminated by an expanded laser beam, and measurements were made of the positions of the resultant diffraction orders. The results (Fig. 3B) are similar to those obtained by microdensitometry. Wedge nonuniformities in film thickness caused frame-specific shifts in the positions of all diffracted orders; this effect was compensated for by measuring the distance between both first orders instead of the position of a single first order.

Minor differences were expected between the results of the on-line diffraction method and the results of the film analysis. Slight movements of the zeroth-order peak may, for example, cause a small change in the band spacing without altering the location of a first-order diffraction peak. Similarly, any augmentation of a diffraction peak by Bragg scattering will affect the film-derived SL. Furthermore, equal weights were attributed to each region of the frame when computing the mean frame SL, whereas for the diffraction process the weights depend on local uniformity of striation spacing.

Some of these effects may have been responsible for the results in plot a of Fig. 3C; here the microdensitometry result shows no clear pause at 17 msec, unlike the on-line diffraction result. On the other hand, plots b and c of Fig. 3C,

corresponding to two subregions of the same film, show that the two subsets of the frame shorten differently; plot c shows agreement with the on-line diffraction record but plot b does not. In this case, some local lateral nonuniformity of contraction was apparent when the film was viewed with a movie projector.

Finally, two intriguing features are present in the data. First, the shortening trace in Fig. 3A shows that a majority of time is spent in the pause state and that only short times, perhaps on the order of the minimum time interval that could be resolved, are required to initiate the subsequent full-velocity shortening. Second, any asynchrony of behavior over the sampled domain will always tend to smooth out any discontinuities present in local, small-volume shortening behavior. These features raise the possibility that the wave forms with the longest pauses and highest burst velocities are the most representative of the molecular events.

The implication of these results is that stepwise shortening behavior extends over many sarcomeres in length and probably over at least several myofibrils

laterally; no cooperative mechanism of this scope has been identified in muscle. Furthermore, the times required for the transition from pause to burst states are too short to be compatible with diffusion processes. It is perhaps more likely that stepwise shortening is the result of cooperative processes taking place over arrays of contractile proteins. If this is so, the change in SL between successive pauses may be quantized in units of, for example, the actin or myosin repeat distances.

M. J. DELAY

N. ISHIDE, R. C. JACOBSON

G. H. POLLACK, R. TIROSH

Department of Anesthesiology and
Division of Bioengineering, University
of Washington, Seattle 98195

References and Notes

1. G. H. Pollack, T. Iwazumi, H. E. D. J. ter Keurs, E. F. Shibata, *Nature (London)* **268**, 757 (1977).
2. R. Rüdél and F. Zite-Ferency, *ibid.* **278**, 573 (1979).
3. T. Iwazumi and G. H. Pollack, *IEEE Trans. Biomed. Eng.* **26** (No. 2), 86 (1979).
4. We thank J. D. Chalupnik for the loan of the camera, R. W. Marvin for technical assistance, and R. Vogel, M. Jacobi, and Y. Hakamori for assistance in the film analysis.

19 November 1980; revised 18 March 1981

Diurnal Rhythm of Cytoplasmic Estrogen Receptors in the Rat Brain in the Absence of Circulating Estrogens

Abstract. *The concentration of cytoplasmic estrogen receptors in the brain of ovariectomized female rats varies during the light-dark cycle. There is no variation in the affinity of the receptors for estradiol, and the rhythm is not due to estrogens from nonovarian sources. Pentobarbital reverses the reduction of receptors that occurs in the dark, and melatonin injection in the light partially mimics the action of darkness in reducing receptor levels. The factors that cause this rhythm in brain estrogen receptors may be one means by which light affects reproductive function.*

Light affects reproduction in at least two ways: (i) in a fixed photoperiod many reproductive events are entrained to the light-dark cycle and (ii) alterations of the photoperiod can change reproductive status. An example of the latter is gonadal regression in rodents that are exposed to a shortened period of light (1). This effect of light is mediated by the pineal gland, possibly by a pineal product that modulates the feedback actions of gonadal hormones in the brain (2). In a fixed photoperiod, events that are entrained to the light-dark cycle in female rats include the luteinizing hormone surge and ovulation (3). This rhythmicity is not eliminated by pinealectomy (4). However, ovariectomized rats show a circadian rhythm in sensitivity to estradiol administered for the induction of sexual receptivity (5); this rhythm is eliminat-

ed by lesions of the suprachiasmatic nuclei, which receive input from visual pathways.

The sensitivity of the brain to estrogens may therefore be modulated by factors that are affected by the light-dark cycle. A change in sensitivity to estrogens could be accomplished by influencing cytoplasmic estrogen receptors, since the initial step in the action of the hormone is to bind to such receptors (6). We now report that estrogen receptors in the brain exhibit a diurnal variation in the absence of circulating estrogens. Consistent with the idea that the diurnal variation may be related to the pineal gland are our findings that (i) levels of estrogen receptors are lower in the dark when the pineal is active, (ii) the decline in the dark period can be blocked by pentobarbital, and (iii) melatonin injec-